New Journal of Physics
An Institute of Physics and Deutsche Physikalische Gesellschaft Journal

Cold dark matter searches at the Canfranc underground laboratory

S Cebrián, E García, D Gonzalez, I G Irastorza, A Morales, J Morales, A Ortiz, A Peruzzi, J Puimedon, M L Sarsa, S Scopel and J A Villar

Laboratorio de Física Nuclear y Altas Energías, Facultad de Ciencias, Universidad de Zaragoza, 50009 Zaragoza, Spain
E-mail: amorales@posta.unizar.es

New Journal of Physics **2** (2000) 13.1–13.20 (http://www.njp.org/)
Received 8 February 2000; online 13 July 2000

Abstract. An overview of the searches for weak interacting massive particles (WIMPs) through detection of their scattering off various target nuclei carried out in the Canfranc Tunnel Astroparticle Laboratory (at 675 and at 2450 metres of water equivalent (m.w.e.)) is given. The main experimental results both for conventional (COSME, IGEX and NaI-32) and for cryogenic detectors (ROSEBUD) are sketched, and a briefing on the forthcoming experiment ANAIS is also presented. The results of a solar axion search are also reported.

1. Introduction

There is substantial evidence [1] that most of the matter of the universe is dark and a compelling motivation to believe that it consists mainly of non-baryonic objects. From the cosmological point of view, two big categories of non-baryonic dark matter have been proposed: cold (weak interacting massive particles (WIMPs) and axions) and hot (light neutrinos) dark matter according to whether they were slow or fast moving at the time of galaxy formation. The general consensus from a variety of observations and well founded theoretical arguments is that a large portion of non-baryonic cold dark matter is needed in the universe. This form of dark matter could be filling the galactic halo in sufficient amounts for one to attempt its detection [2].

The direct detection of WIMPs relies on the measurement of their elastic scattering off the target nuclei in a suitable detector [3, 4]. Slow moving ($\simeq$300 km s^{-1}) and heavy (10–10^3 GeV) WIMPs pervading the galactic halo could, for instance, make a Ge nucleus recoil with a few keV (only about a quarter of this energy is visible in the detector), at a rate which depends on the type of WIMP and interaction. Because of the low interaction rate and the small deposition of energy, the direct search for particles of dark matter through their scattering by nuclear targets requires ultralow background detectors with very low energy thresholds. Moreover, the (almost)

1367-2630/00/000013+20$30.00

exponentially decreasing shape of the predicted nuclear recoil spectrum mimics that of the low-energy background registered by the detector. All these features together make WIMP detection a formidable experimental challenge.

Customarily, one compares the predicted event rate with the observed spectrum. If the former turns out to be larger than the measured one, the particle under consideration can be ruled out as a dark matter component. Such non-appearance of the WIMP is expressed as a contour line $\sigma(m)$ in the plane of the WIMP–nucleus elastic scattering cross section versus the WIMP mass m, which excludes, for each m, those particles with cross-sections above the contour line $\sigma(m)$ because such values give a rate above the observed spectrum.

This mere comparison of the expected signal with the observed background spectrum (which itself mimics the signal) is not supposed to detect the tiny imprint left by the dark matter particle, but only to exclude or constrain ranges of parameters. A convincing proof of the detection of a WIMP would be to find unique signatures in the data characteristic of the WIMP, such as seasonal [5] (or other) asymmetries, provided that they are not faked by the background or by instrumental artefacts. The reliability of such identification techniques is at present being discussed.

The Canfranc Dark Matter Searches programme is attempting to detect this type of non-baryonic dark matter directly, through the nuclear recoil in WIMP-nucleus scattering. To this end various strategies are being followed. On the one hand, several nuclear targets are used. On the other, conventional detectors (such as semiconductor diodes (Ge) and scintillators (NaI)), as well as thermal detectors operating at low temperature (such as sapphire bolometers), are being employed. The main goal being pursued in the Canfranc programme is the search for genuine signatures of dark matter, such as the annual modulation [5] of the WIMP signal due to the June–December variation of the relative Earth–halo velocity and the dependence of the detection rate on the nuclear target. The first type of signature is being investigated mainly with large masses of scintillators, whereas the mass number A or spin J nuclear target dependence is being addressed by means of cryogenic devices.

A search for solar axions in Canfranc with a small Ge detector through their Primakoff conversion into photons in the crystalline lattice of the detector has recently been undertaken.

In the following, we will review the status, results and prospects of the experiments performed in the Canfranc Tunnel Astroparticle Laboratory in searching for WIMPs and axions.

2. Germanium experiments

A Ge detector using germanium of natural abundances of isotopes (COSME) of the Universidad de Zaragoza–University of South Carolina–PNNL collaboration and another one (RG-II) made of enriched ^{76}Ge of the International Germanium Experiment on Double Beta Decay (IGEX) collaboration are being used in Canfranc to search for WIMPs interacting coherently with the Ge nuclei of the detectors.

The COSME detector [6] is a p-type coaxial hyperpure natural germanium crystal with a mass of 234 g which has a long term resolution of 0.43 keV full width at half maximum (FWHM) at 10.37 keV. The detector is placed within a shielding of 10 cm of 2000-year-old (Roman) lead (inner layer) plus 20 cm of low activity lead (about 70 years old). A 3 mm thick PVC box sealed with silicone closes the lead shielding to purge the radon gas. The PVC box is covered by 1 mm of cadmium and 20 cm of paraffin and borated polyethylene. All the shielding and mounting is supported by 10 cm of vibrational and acoustic insulator sandwiched within two 10 cm layers of wood mounted on a floor of concrete (20 cm). It was first operated [6] in

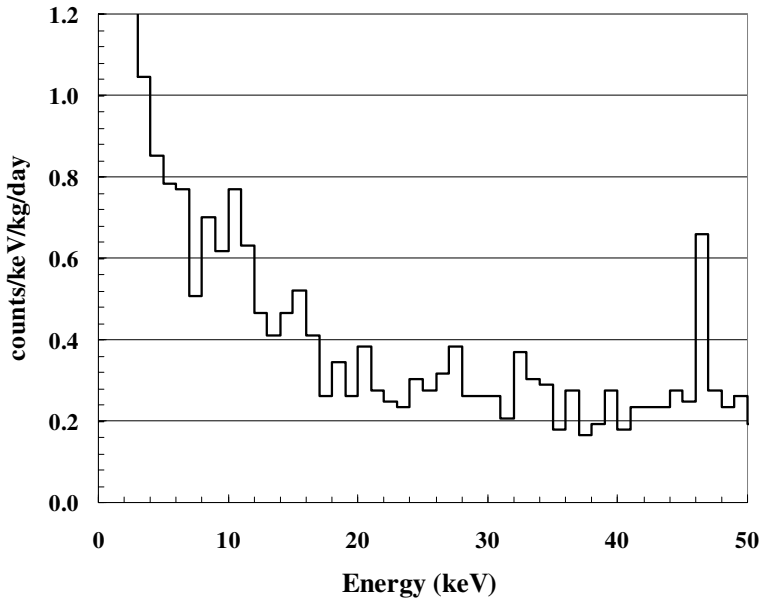

Figure 1. The low-energy background spectrum of COSME-2.

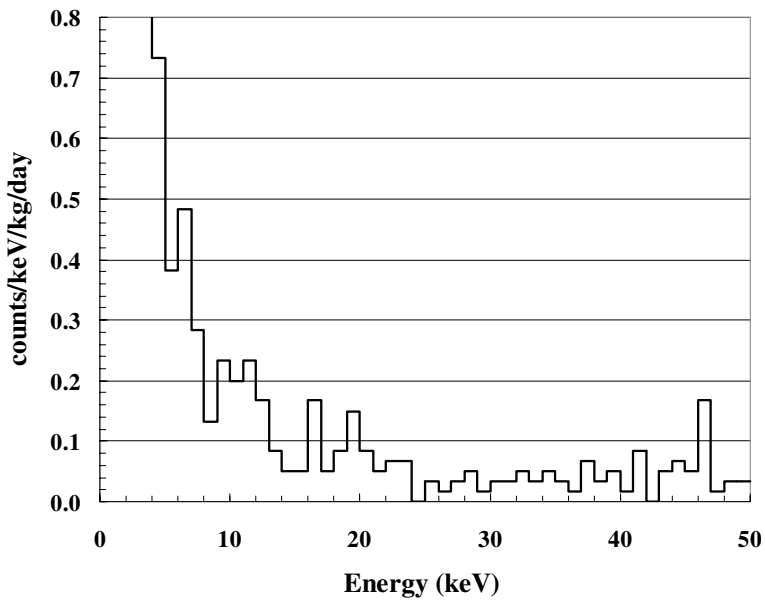

Figure 2. The low-energy background spectrum of RG-II.

the former Canfranc underground facility at 675 m.w.e. in a small gallery of a closed railway tunnel in the Spanish Pyrenees. In that set-up, the energy threshold was $\mathrm{E}_{thr} = 1.6$ keV and the background at threshold was about 10 counts keV^{-1} kg^{-1} day^{-1}. To derive the exclusion plots $\sigma(m)$, the predicted signal is required to be not larger than the 90% confidence level upper limit of the Poissonian background counts recorded in a chosen energy bin. In the derivation of the interaction rate signal, it is supposed that the WIMPs form an isotropic, isothermal non-rotating halo of density $\rho = 0.3$ GeV cm^{-3} and have a Maxwellian velocity distribution with

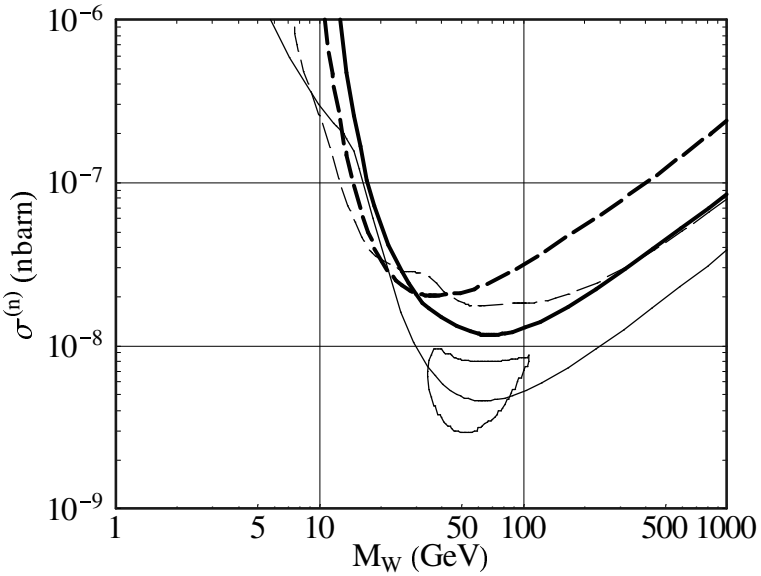

Figure 3. Exclusion plots from COSME-2 (thick broken line) and IGEX data (thick full line), compared with the combined Ge limit (thin broken line) and with that of the DAMA (NaI-0) experiment (thin full line). The closed contour is the region singled out by the annual modulation effect reported by the DAMA collaboration.

$v_{\rm rms} = 270$ km s^{-1} (with an upper cut-off corresponding to an escape velocity of 650 km s^{-1}), and a relative Earth–halo velocity of $v_{\rm r} = 230$ km s^{-1}). In the COSME-1 data, the energy range chosen to derive the exclusion plot was 1.6–8 keV where the background was, approximately, 5 counts keV^{-1} kg^{-1} day^{-1}. In spite of this modest figure, the results after 130 kg day of exposure improved the exclusion plots at low masses (9–20 GeV) obtained with other Ge experiments because of the low threshold energy of COSME-1.

The COSME detector has been reinstalled, in better background conditions (at 2450 m.w.e.) inside a Marinelli beaker in Roman lead (COSME-2) in the same shielding as that used for the three 2.1 kg enriched germanium detectors of IGEX (the International Germanium Experiment on Double Beta Decay) [7]. A recent upgrading of these enriched detectors allows one to use them also in WIMP searches. The new shielding of COSME has an inner cubic block (2.5 tons) of Roman lead (2000 years old), of dimensions 60 cm $\times$ 60 cm $\times$ 60 cm, with the detectors fitted into precision-machined holes, to minimize the empty space around the detectors available to radon. In fact, there is no empty space left between the Ge detectors and the lead cube, except for the matching of the lead bricks. The Roman lead block is within a cube of 1 m sides of low activity lead ($\simeq$70 years old). There is 15–20 cm of Roman lead between any part of the detector and the outer cube of lead. Then a 2 mm-thick cadmium sheet surrounds the external lead shield and two layers of PVC seal the enclosure to prevent the intrusion of radon. The remaining radon gas is eliminated from the inside by forced circulation of the evaporated nitrogen in the tightly closed enclosure, bringing it down to the level of 25 μBq l^{-1} from an average of 50 mBq l^{-1} existing in the forced air ventilated underground laboratory. Neutron shielding and an active muon veto cover the sides of the IGEX–COSME experimental setup, except for the side where the detector's Dewar flasks are located. In its new installation, COSME-2 has an energy threshold

of $E_{thr} = 3$ keV and an energy resolution of $\Gamma(\mathrm{FWHM}) = 0.4$ keV at 10 keV. The average background rate, in 311 days of exposure ($Mt = 72.8$ kg days) is 0.6 counts keV^{-1} kg^{-1} day^{-1} from the range 2–15 keV and 0.3 counts keV^{-1} kg^{-1} day^{-1} from the range 15–30 keV. The COSME-2 spectrum is shown in figure 1.

One of the 2.1 kg Ge IGEX detectors (with an energy threshold of 4 keV) is also taking data for WIMP searches in the same shielding. The preliminary results, corresponding to 30 days of analysed data ($Mt = 60$ kg days) provide the background rates of $\simeq$0.1 counts keV^{-1} kg^{-1} day^{-1} averaged between 4 and 10 keV, $\simeq$0.07 counts keV^{-1} kg^{-1} day^{-1} in the region 10–20 keV and less than 0.05 counts keV^{-1} kg^{-1} day^{-1} between 20 and 40 keV. Figure 2 shows the background spectrum obtained with the IGEX RG-II detector. The taking of data with an improved background below 20 keV is in progress. The exclusion plots from the COSME and IGEX preliminary data are shown in figure 3, in comparison with the previous Ge results combined, as well as with that of the DAMA experiment. All the exclusion plots, including that of the other previous Ge [6],[8]–[12] and NaI [13] experiments, have been recalculated from their respective original spectra with the same set of hypothesis and parameters as those used for IGEX and COSME. Notice that the last Heidelberg–Moscow data [11] have been included in the combined Ge exclusion limit. The closed contour is the region singled out by the annual modulation effect reported by the DAMA collaboration (corresponding to runs NaI-1, and NaI-2) [14].

3. The Canfranc sodium iodide dark matter searches

Other suitable nuclear targets for use as WIMP scatterers are sodium and iodine. The 100% isotopic contents of A-odd isotopes of NaI scintillators (^{127}I and ^{23}Na, respectively) make them sensitive also to spin-dependent interactions with WIMPs. A search for WIMPs with a set of sodium iodide scintillators of total mass 32.1 kg was carried out in a pilot experiment (NaI-32) to assess the capability of such scintillators and to set up the conditions for a larger experiment. The main objective of the experiment [15] was to look for the annual modulation of the WIMP signal [5]. It is well known that the yearly modulation occurs because of the seasonal variation in the relative velocity of the Earth and the galactic halo due to the Earth's rotation around the Sun. The Sun moves around the galaxy at a velocity of 232 ± 20 km s^{-1} and the Earth moves around the Sun with an orbital speed of 30 km s^{-1} in an orbit whose axis makes an angle of $\delta = 30.7^{\circ}$ with respect to the vector velocity of the Sun. The resulting net speed of the Earth with respect to the halo reference frame oscillates between about 245 km s^{-1} in June and 215 km s^{-1} in December, and so the maximum amount of energy that can be deposited in the detector by the WIMPs and their detection rates change accordingly. Consequently, an annual oscillation of the dark matter signal should appear [5, 16]. Various experiments have searched for this type of signature [14, 15],[17]–[20].

The detector set consisted of three NaI scintillators made by BICRON. Each crystal (with a regular hexagonal cross-section of 8.0 cm each side and a height of 20.3 cm) has a mass of 10.7 kg. The shielding was formed by 20 cm of low activity lead and a few inner oxygen-free high conductivity (OFHC) copper sheets ($\simeq$6 mm thick). A PVC box (silicone sealed) closed tightly the shielding which was surrounded by 1 mm of cadmium and 20 cm of paraffin and borated polyethylene. All the shielding and mounting was placed over plates of vibrational and acoustic insulator sandwiched between two layers of 10 cm wood on a 20-cm thick concrete floor. The experimental set-up was placed in one of the rooms of the former Underground Laboratory

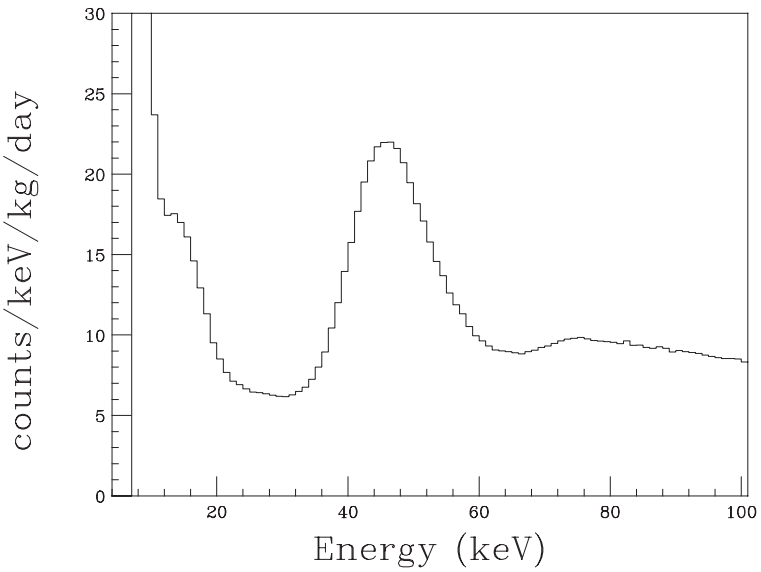

Figure 4. The low-energy spectrum of the sodium iodide experiment NaI-32.

of the Universidad de Zaragoza, in the Canfranc Tunnel (in the Spanish Pyrenees) at a depth of 675 m.w.e. [15].

The experimental parameters of this experiment were as follows. The overall energy resolution was 9% at 511 keV and 30% at 46.5 keV. The energy threshold stood at about 8 keV of visible energy and the differential rate at the energy windows used in the analysis (from 9 to 28 keV) ranged from 16 to 8 counts $\mathrm{keV}^{-1}\ \mathrm{kg}^{-1}\ \mathrm{day}^{-1}$. The data taking of the NaI-32 experiment extended over a period of about two years. The exposure used in the analysis to derive exclusion plots from the total time-integrated observed rate was 4613.6 kg days.

From the spectrum of figure 4 corresponding to the total time-integrated registered rate, $\sigma(m)$ exclusion plots have been derived. They are shown as broken lines in figures 5 and 6, for, respectively, the coherent and spin-dependent cases. The plotted cross-sections are point-like. The quenching factors used here are $Q(^{23}\mathrm{Na}) = 0.4 \pm 0.2$ and $Q(^{127}\mathrm{I}) = 0.05 \pm 0.02$, taken from [21]. The corresponding coherent and spin nuclear form factors were taken into account in the derivation of the rates, assuming Fermi form factors for the coherent case. For the spin case, unity has been taken for ^{23}Na ($J = \frac{3}{2}$) whereas for ^{127}I ($J = \frac{5}{2}$) we have assumed the same as for ^{131}Xe [22]. The $\lambda_p^2\ J(J+1)$ factors for ^{23}Na and ^{127}I were taken, respectively, to be 0.041 (from the odd group model [23]) and 0.023 (from the interacting boson model [24]). More details can be found in [15].

To analyse the possible annual modulation of the signal, 1342.8 kg days of data (corresponding to the exposures of June minus December in two years with 21.4 kg of NaI) were used. The data did not reveal any difference between the rates of June and December, which one would expect from the fact that the Earth–halo relative velocity is faster in June than it is in December. The absence of such a modulation effect resulted in constraints on cross-sections and masses of spin-dependent and spin-independent interactions of WIMPs more stringent than those obtained from the customary method of comparing the total expected rate with that recorded in a given energy region, integrated over the whole exposure time. The exclusion plots obtained with the modulation method are also shown in figures 5 and 6 as full lines. The constraints obtained

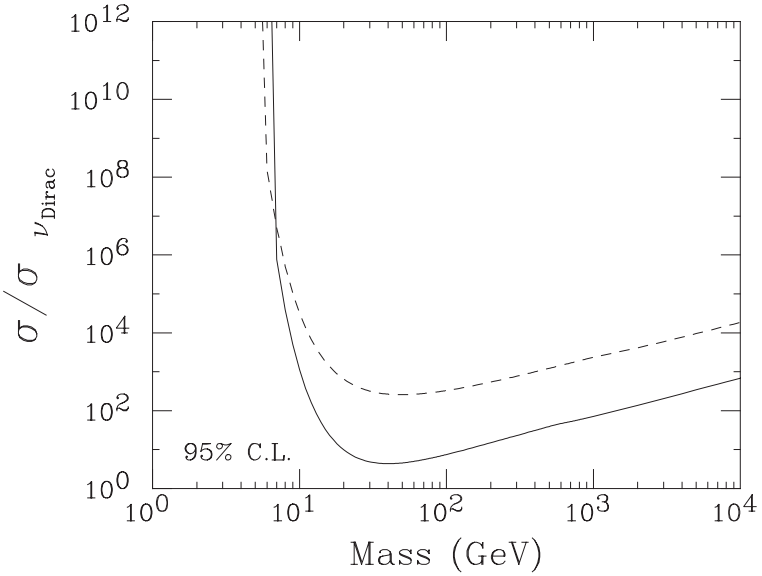

Figure 5. Exclusion plots for coherent interactions obtained in the experiment NaI-32. The broken line refers to the standard method of exclusion whereas the full line corresponds to the annual modulation analysis.

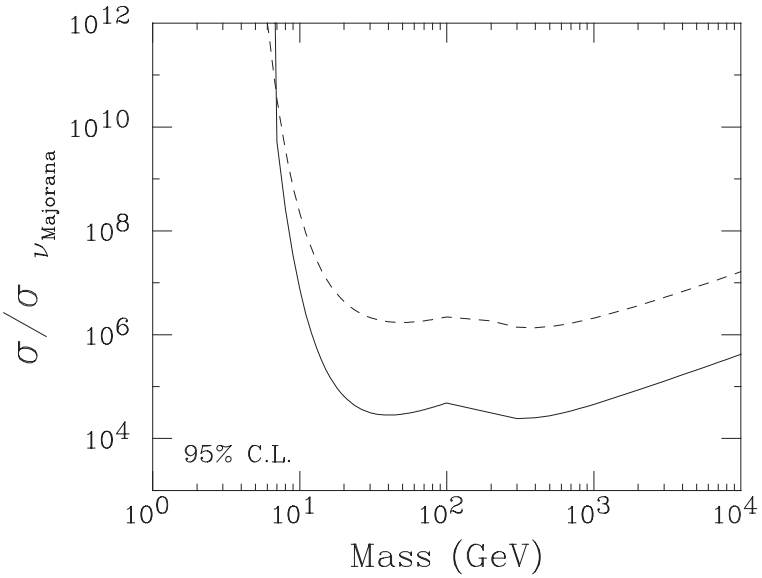

Figure 6. The same as in figure 5 but for spin-dependent interactions.

with the annual modulation search (time variation of the rate) improve on those obtained with the conventional (total time-integrated rate) method. A complementary analysis intended to discover a possible periodic component in the NaI-32 data recorded by two detectors for 424 days (the so-called modulation significance method) [16] also gave a null result [15].

A larger experiment, Annual Modulation Search with NaIs (ANAIS), with 107 kg of NaI scintillators is now being installed at 2450 m.w.e., to pursue the search for annual modulation of WIMPs initiated by NaI-32. ANAIS [4] consists of ten hexagonal NaI crystals (each of

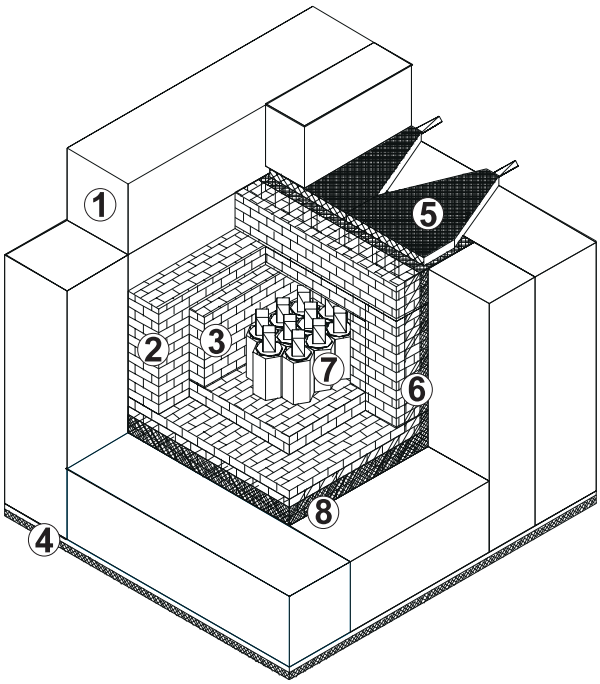

Figure 7. A schematic view of the ANAIS experimental set-up. 1: 40 cm of neutron shielding; 2: 20 cm of lead; 3: 10 cm of Roman lead; 4: vibration insulation; 5: 2×0.5 m^2 muon veto; 6: PVC box; 7: 10×10.7 kg of NaI; and 8: 2 mm of Cd.

mass 10.7 kg) of the type used in the NaI-32 experiment mentioned above, recently upgraded to provide low radioactivity and a better energy threshold. They are within an electroformed double box of copper and Roman lead, and are coupled through light guides to ultralow background photomultipliers placed outside the internal shielding and cooled through Peltier devices. The shielding consists of 10 cm of Roman lead, 20 cm of low-activity lead, 2 mm of cadmium and 20–40 cm of polyethylene and water. It is sealed in a box made of PVC maintained at overpressure by the injection of 200 l h^{-1} of N_2 to prevent the intrusion of radon. An active muon veto covers the set-up. A schematic view of the forthcoming ANAIS experimental set-up can be seen in figure 7.

The acquisition system records the events fired in each crystal, registering their energies and times (to within an accuracy of better than 1 s throughout the experiment). Anticoincidence pulses are recorded with digitizers for pulse shape discrimination. Monitoring and stabilization control of the experimental parameters (which is essential for modulation searches) will be performed particularly carefully. The expected performances are an energy threshold of $\simeq$2 keV, and a background of about 2–4 counts keV^{-1} kg^{-1} day^{-1} in the low-energy region. Results from preliminary tests of the performances of scintillators and optimization of the background conditions are encouraging. A running test with a smaller set-up is under way.

Measurement of the radiopurity of the ANAIS components has been carried out with an ultralow background high-purity germanium (HPGe) detector in Canfranc. The Monte Carlo estimate of the expected background spectrum obtained by using the measured level of radioactive contamination as input is shown in figure 8. From this estimated background, projected exclusion

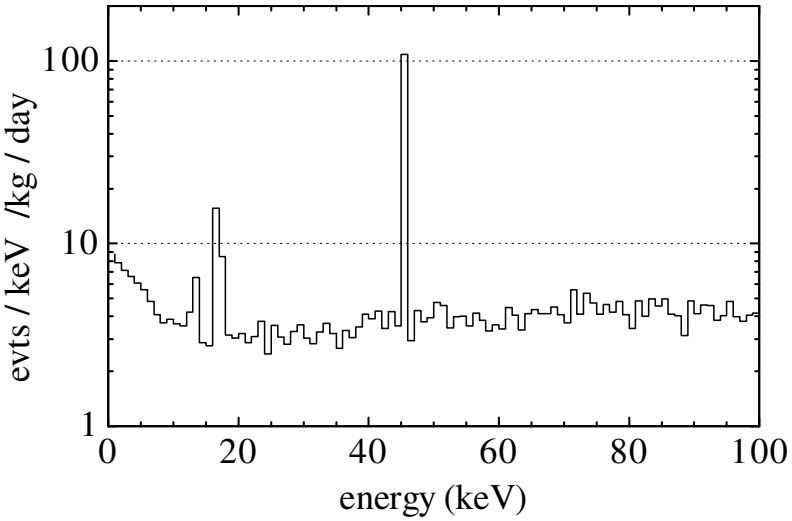

Figure 8. The Monte Carlo estimated background of the ANAIS set-up.

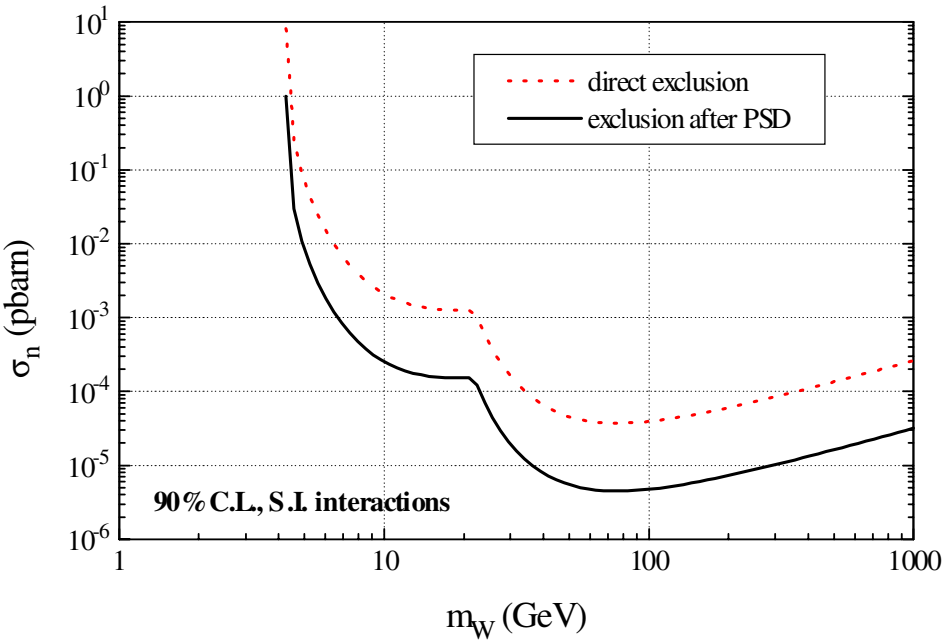

Figure 9. The sensitivity of the ANAIS set-up for an exposure of 107 kg years, a threshold of 2 keV and a background of 2 events keV^{-1} kg^{-1} day^{-1} in terms of the spin-independent exclusion plots.

plots have been derived under the same set of hypotheses and halo parameters as those used throughout this work. Figure 9 shows, for instance, the $\sigma^n(m)$ plot for spin-independent WIMP–nucleon interaction. The curve labelled PSD refers to the case in which statistical pulse shape discrimination (PSD) of the background has been used to reduce the nuclear recoil background from 15% to 1% of the measured background spectrum, for energies from 2 to 20 keV, as discussed in [25]. The potential of ANAIS for annual modulation searches is given in [26].

4. The Canfranc dark matter search with cryogenic detectors

As is well known, thermal detectors [27] use the energy deposition of WIMPs more efficiently than do the conventional ionization detectors because most of the nuclear recoil energy in WIMP scattering goes to heat. They are true low-energy detectors, for which the visible energy is practically the whole recoil energy (a quenching factor close to unity). Moreover, the mechanisms and quanta involved in the physics of the detection imply that they should have better energy thresholds and energy resolution than do the conventional ionization detectors. In particular, the energy resolution on nuclear recoils achieved by the sapphire bolometers used in Canfranc (see below) is better than that obtained with the HPGe detector COSME, which is a detector of very good energy resolution ($\Gamma(10\ \mathrm{keV}) = 0.4\ \mathrm{keV}$). Such cryogenic detectors are very well suited for detecting low mass WIMPs ($m \leq 10$ GeV) and offer the possibility of using different targets to tune the sensitivity for different WIMP masses. Finally, they can discriminate the background (electron recoils) from nuclear recoils by collecting at the same time the charge (or light) produced by the ionizing component of the deposited energy (hybrid detection) [28, 29], allowing further improvements in sensitivity. Although the radio-impurity of the bolometers is still higher than that of HPGe, notable improvements are being accomplished.

A WIMP search with small sapphire bolometers, called Rare Objects SEarch with Bolometers UndergrounD (ROSEBUD) is being carried out in Canfranc (at 2450 m.w.e.) with the purpose of detecting the scattering of WIMPs off Al and O nuclei. The experiment is a collaboration of the Universidad de Zaragoza and the Institute d'Astrophysique Spatiale (IAS Orsay). It features three small sapphire bolometers with Ge neutron transmutation doped (NTD) thermistors to measure the increase of temperature produced by the particle interaction in the crystal. The system is cooled down to 20 mK in a dilution refrigerator placed in the ultralow radioactivity environment of the underground laboratory.

The first phase of the experiment consists of two 25 g (B175 and B200) and one 50 g (B213) selected sapphire bolometers operating inside a small refrigerator (stick type, 6 cm diameter, 100 cm long) at 20 mK. B200, mounted on top of the set, is a composite bolometer (25 g sapphire and 2 g of LiF enriched in ^{6}Li to 96% glued as absorbers) [30] to monitor the thermal and fast neutron background of the laboratory. A cylinder (34.5 mm diameter and 30.8 mm high) of Roman lead is placed below B200 to screen the two lower sapphire absorbers from radioactivity in the components of the dilution unit. Figure 10 shows a schematic view of the bolometers inside the dilution refrigerator in the first experimental set-up.

The shielding of the ROSEBUD device consists of an inner shielding located inside the dilution unit at helium bath temperature, made of a liner of Roman lead (4 mm thick) surrounding the bolometers to shield the intrinsic radioactivity of the 0.5 mm thick stainless steel walls of the inner vacuum chamber and a 14.4 mm thick high purity copper wall to shield the radioactivity of the outer Dewar flask. The ancient (2000-year-old) Roman lead of the shielding has very low contamination ($<$10 mBq kg^{-1} from ^{210}Pb, $<$0.2 mBq kg^{-1} from ^{238}U and $<$0.3 mBq kg^{-1} from ^{232}Th). The external shielding (at room temperature) consists of 10 cm of Roman lead bricks, 15 cm of low-activity lead (30 Bq kg^{-1} from ^{210}Pb), a 1 mm cadmium foil and a mu-metal screen plus a plastic box which tightly contains the enclosure. A layer of 20 cm of borated water will be added to screen neutrons. The experimental set-up is installed within a Faraday cage and an acoustic isolation cabin, supported by an antivibration platform. A diagrammatic view of the experimental set-up of ROSEBUD is given in figure 11.

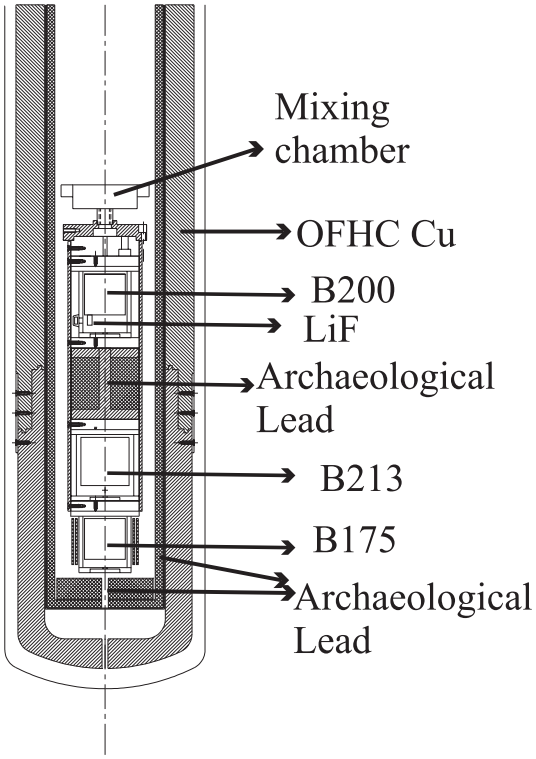

Figure 10. A schematic view of the bolometer block of ROSEBUD.

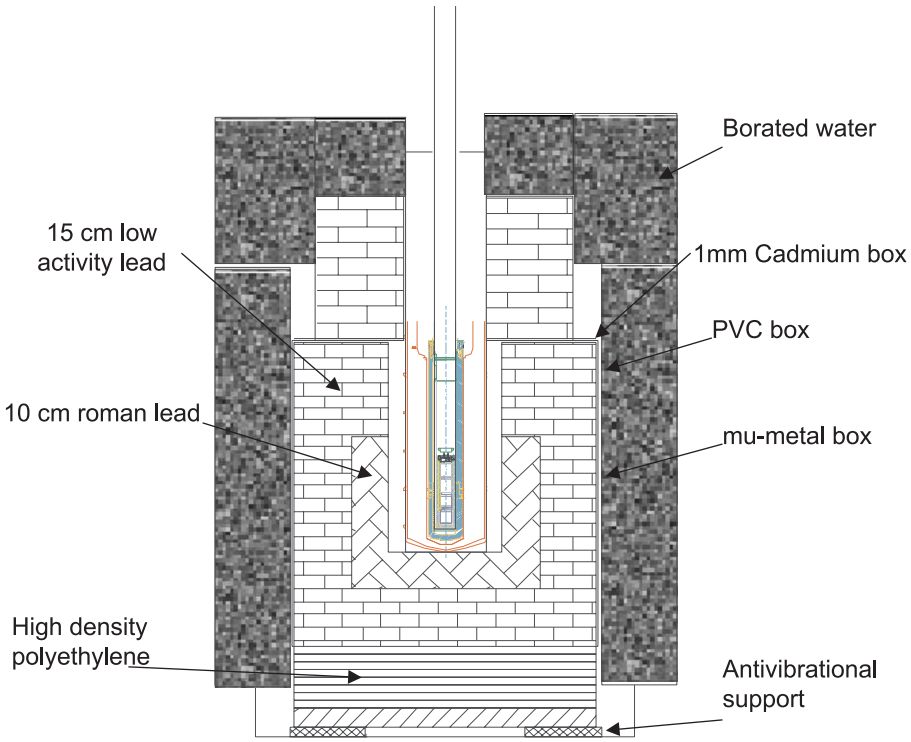

Figure 11. A schematic view of the ROSEBUD set-up.

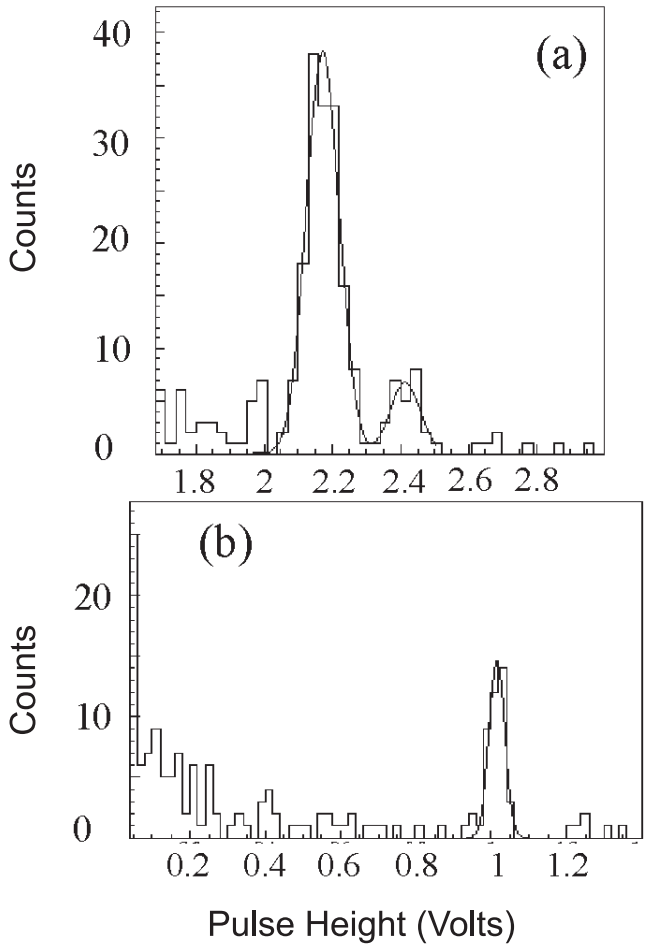

Figure 12. Calibration spectra in B175: (a) a ^{57}Co source (122 and 136 keV lines) and (b) a ^{241}Am source (60 keV line).

The power supply inside the cabin is provided by batteries and data transmission from the cabin through convenient filters is based on optical fibres. Pumps have vibration-decoupled connections.

Infrared (IR) pulses are periodically sent to the bolometers through optical fibres in order to monitor the stability of the experiment. The resulting heat pulses are a useful means of correcting any sensitivity drift of the bolometers during the experiment. A FWHM resolution of 2.4 keV corresponded to this pulser line in a short measurement, increasing to 3 keV after a whole night of measurement. In the first background tests, the energy corresponding to these pulses was set up typically in the interval 100–200 keV. In the final runs, it will be adjusted to lower energies, in the region where the dark matter analysis makes sense. The corresponding pulses are quite similar in shape to the background or ^{57}Co source events, but slightly faster.

For absolute energy calibration of the two bolometers placed at the bottom of the cryostat during the background tests external ^{57}Co and ^{241}Am sources are used. Figure 12 shows the calibration spectra for both sources. The three lines (60 keV (^{241}Am), 122 keV and 136 keV (^{57}Co)) allow one to extrapolate (assuming a linear response) the calibration to lower energies. For the calibration of the upper bolometer, an internal ^{241}Am source has been used. Its alpha

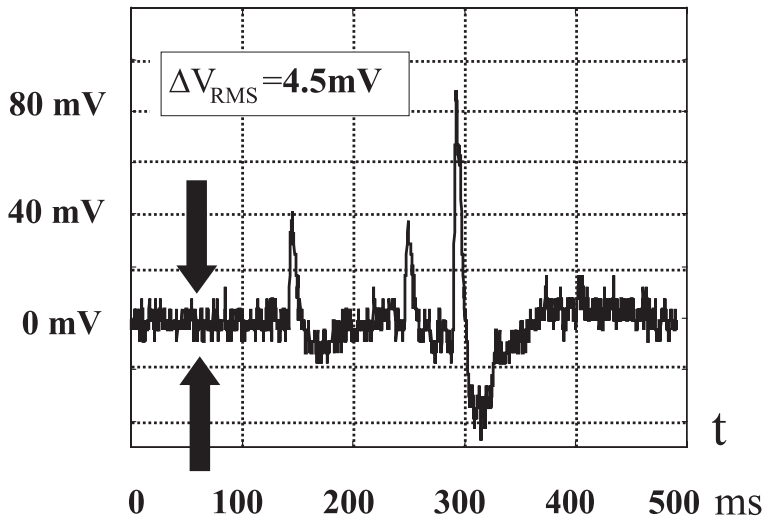

Figure 13. Low-energy pulses from B213 during the first ROSEBUD run at Canfranc. 100 mV corresponds to about 5 keV.

emission (5.5 MeV) has been degraded by mylar foils in order to leave clean the region where the neutron signal (above the Q value of the ^{6}Li(n,α) reaction, 4.78 MeV) should be found.

The bolometers are suspended inside an OFHC copper frame (coupled to the mixing chamber of the dilution refrigerator) by Kevlar wires tensioned to drive the mechanical resonance frequency to the highest possible value. The first tests in Canfranc have shown that the microphonic and electronic noise level is quite good, about 2 nV Hz$^{-1/2}$ below 50 Hz.

The bolometers had been tested previously in Paris (at the IAS) and shown to give very good performances [31], a FWHM energy resolution $\Gamma(1.5\ \mathrm{keV}) = 120$ eV and an energy threshold of about 300 eV). Typical sensitivities obtained (in Canfranc) are in the range 0.3–1 μV keV^{-1}. Overall resolutions of 3.2 and 6.5 keV FWHM were typically obtained with B213 and B175, respectively, at 122 keV. With B175, 2.8 keV FWHM was obtained at 60 keV. Typical pulses have decay and rise times in the ranges 2–4 ms and 600–1300 μs, respectively. Some low-energy background pulses in bolometer 213 can be seen in figure 13. They correspond to energies below 5 keV.

In the bolometer made of sapphire and LiF, two types of pulses can be clearly identified (see figure 14), corresponding to interactions in sapphire (the background can also be distinguished from IR events) and interactions in LiF coming mainly from the ^{241}Am source (slower events). This event recognition is very interesting for neutron measurements.

Radiopurity measurements of some of the ROSEBUD internal components (NTD sensors, sapphire crystals, copper frames etc) were carried out at the underground laboratories of Modane (LSM) and Canfranc using ultralow background germanium detectors [32]. The upper limit on the total background counting rate produced by the radio-impurities of the ROSEBUD components was estimated to be about 5 counts keV^{-1} kg^{-1} day^{-1}. This rate is still one to two orders of magnitude larger than that obtained in good germanium detectors.

ROSEBUD is performing a series of short runs under various conditions (of durations of a few days each) to optimize the background, minimize the microphonics noise and improve the performances of the bolometers, before going to longer running times.

We obtained a background as large as 120 counts keV^{-1} kg^{-1} day^{-1} in a preliminary testing measurement at around 100 keV, after the installation of the external shielding. To

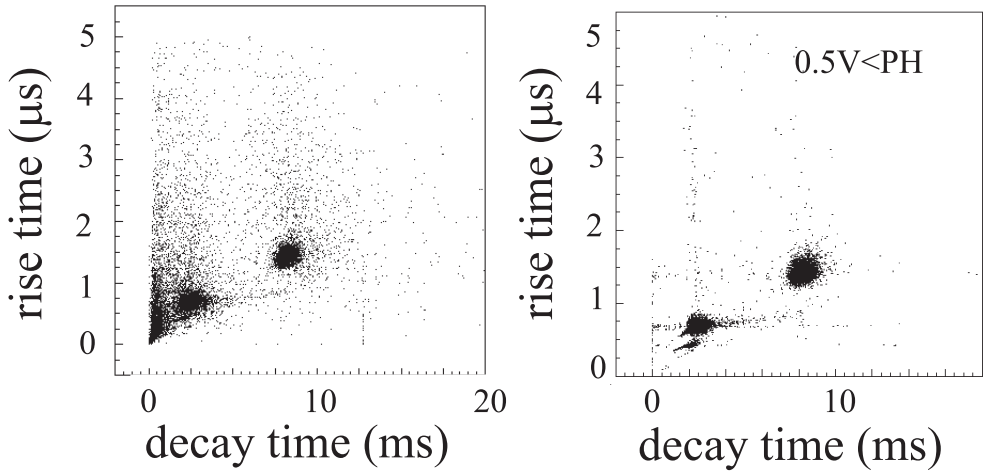

Figure 14. Discrimination between interactions in LiF (slower pulses) and in sapphire (IR events can also be distinguished) according to their rise and decay times. It improves clearly for pulses larger than 0.5 V.

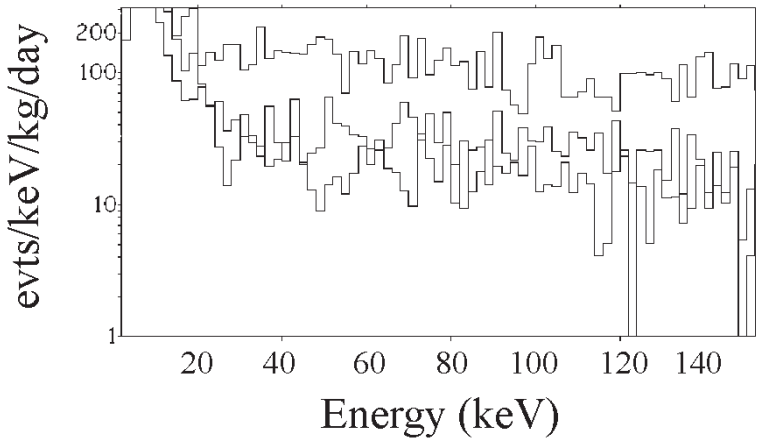

Figure 15. Successive background spectra of ROSEBUD obtained after replacement of several components.

understand and reduce this background, several components of the cryostat (multilayer insulators, activated charcoal traps etc) have been measured in the ultralow background HPGe testing bench at Canfranc. After subsequent modifications in the cryostat, a background level of about 30 counts keV^{-1} kg^{-1} day^{-1} at around 100 keV was obtained in bolometers B175 and B213. Further reductions of the internal background have been achieved by replacing some other internal pieces of the cryostat and cleaning more efficiently the contribution of radon coming from cryogenic liquids and/or the inner cavity. The current level stands now at about 20 counts keV^{-1} kg^{-1} day^{-1} in the 50–100 keV region. Figure 15 shows the successive background spectra obtained in the running tests. Improving the background by one more order of magnitude is the current objective of ROSEBUD. To this end, independent measurements of the radiopurities of individual components (including the steel cryostat) are being performed and then they are removed when necessary.

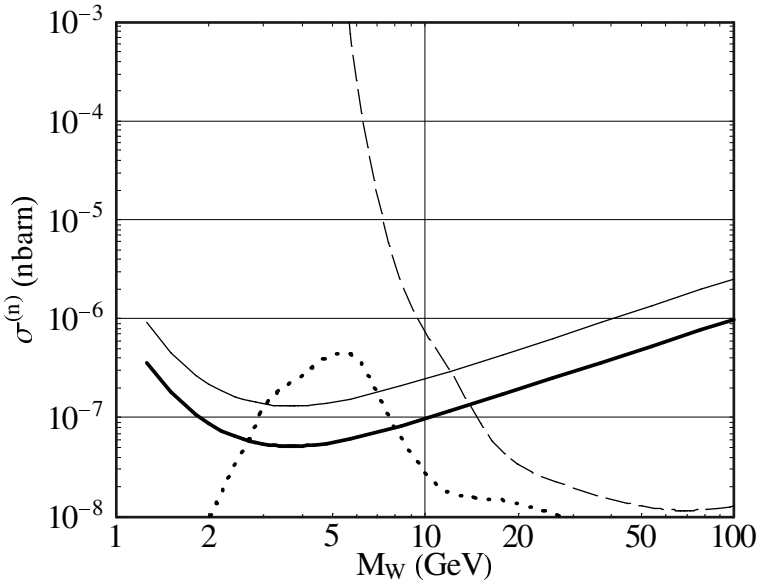

Figure 16. Expected $\sigma(m)$ exclusion plots of the ROSEBUD experiment for spin-independent coupling (assuming a flat background of 1 counts keV^{-1} kg^{-1} day^{-1}, a threshold of 300 eV and an energy resolution of 100 eV).

The expected exclusion plots (90%) of ROSEBUD for spin-independent coupling of neutralinos to ordinary matter obtained by assuming a flat background of 1 count keV^{-1} kg^{-1} day^{-1}, a threshold energy of 300 eV and a FWHM resolution of 100 eV in the low-energy region are shown in figure 16. In the case of bolometric detectors the quenching factor (nuclear versus electron recoil efficiency) is practically unity (0.98 ± 0.05 for sapphire bolometers measured at 100 keV recoil energy [33]). For the coherent case a Fermi form factor has been used. The exclusion plots have been normalized with respect to the neutralino–nucleon cross-section. Two curves are shown corresponding to the results from one bolometer made of 50 g of Al_2O_3 operating for 30 days (the thin full line) and for one year (the thick full line). The dotted line represents the theoretical prediction for the neutralino–nucleon cross section provided by an unconstrained minimal supersymmetric standard model (MSSM) in which the usual GUT relations among gaugino masses are relaxed [34]. For comparison, the envelope of the existing exclusion curves derived from the various Ge experiments [6],[8]–[11] (and that of this work) is also shown (the thin broken line). It can be seen that the expected sensitivity of ROSEBUD will allow one to detect neutralino configurations lighter than 10 GeV.

The next step of the ROSEBUD programme is to continue the improvement of the background by removing the radio-impure components and controlling the ingress of radon. Then two different bolometers, one made of 50 g of sapphire and one of 60 g of germanium, operating together will investigate the target dependence of the WIMP rate. As a further step in this line of research, the use of two medium-sized bolometers, made of 200 g of Al_2O_3 (which is now ready) and a 168 g germanium crystal (which is being prepared) is foreseen.

5. Axion searches in Canfranc

The axion, introduced 20 years ago as the Nambu–Goldstone boson of the Peccei–Quinn symmetry to explain in an elegant way CP conservation in QCD [35], is remarkably also one of the best candidates to provide at least a fraction of the non-baryonic dark matter of the Universe. A combination of astrophysical and nuclear physics constraints and the requirement that the axion relic abundance does not overclose the Universe restrict the allowed range of viable axion masses to relatively narrow windows [36]–[38]:

$$10^{-6}\ \mathrm{eV} \lesssim m_a \lesssim 10^{-2}\ \mathrm{eV} \qquad \text{and} \qquad 3\ \mathrm{eV} \lesssim m_a \lesssim 20\ \mathrm{eV}. \tag{1}$$

The physical process used in axion search experiments is the Primakov effect. It makes use of the coupling between the axion field ψ_a and the electromagnetic tensor:

$$\mathcal{L} = -\tfrac{1}{4} g_{a\gamma\gamma} \psi_a \epsilon_{\mu\nu\alpha\beta} F^{\mu\nu} F^{\alpha\beta} = -g_{a\gamma\gamma} \psi_a \vec{B} \cdot \vec{E} \tag{2}$$

and allows the conversion of the axion into a photon. Solid state detectors provide a simple mechanism for axion detection [39, 40]. Axions can pass in the proximity of the atomic nuclei of the crystal where the intense electric field can trigger their conversion into photons. In the process the energy of the outgoing photon is equal to that of the incoming axion.

Axions can be efficiently produced in the interior of the Sun by Primakov conversion of the blackbody photons in the fluctuating electric field of the plasma. The resulting flux has an outgoing average axion energy E_a of about 4 keV (corresponding to the temperature in the core of the Sun, $T \simeq 10^7$ K) that can produce detectable x-rays in a crystal detector. Depending on the direction of the incoming axion flux with respect to the planes of the crystal lattice, a coherent effect can be produced when the Bragg condition is fulfilled, leading to a strong enhancement of the signal. A correlation of the expected count rate to the position of the Sun in the sky is a distinctive signature of the axion which can be used, at the very least, to improve the signal-to-background ratio.

The process described above is independent of m_a and so are the achievable bounds for the axion–photon coupling $g_{a\gamma\gamma}$. This fact is particularly appealing, since other experimental techniques are limited to a more restricted mass range: 'haloscopes', that use electromagnetic cavities to look for the resonant conversion into microwaves of non-relativistic cosmological dark halo axions, do not extend their search beyond $m_a \simeq 50\ \mu$eV, while the dipole magnets used in 'helioscope' experiments are not sensitive to solar axions heavier than $m_a \simeq 0.03$ eV.

A pilot experiment carried out by the SOLAX collaboration [41] has already searched for axion Primakov conversion in a germanium crystal of mass 1 kg obtaining the limit $g_{a\gamma\gamma} \lesssim 2.7 \times 10^{-9}\ \mathrm{GeV}^{-1}$. In much the same way, data from the COSME-2 germanium experiment, currently running in Canfranc, have been analysed for the detection of solar axions, because of the favourable low-energy threshold (2 keV) and good background of such a detector [42]. The results, after an exposure of 311 days, lead to a similar bound for the axion–photon coupling $g_{a\gamma\gamma} < 2.8 \times 10^{-9}\ \mathrm{GeV}^{-1}$. These are the (mass independent but solar model dependent) most stringent laboratory bound for the axion–photon coupling obtained so far, although they are less restrictive than the globular cluster bound [43] $g_{a\gamma\gamma} \lesssim 0.6 \times 10^{-10}\ \mathrm{GeV}^{-1}$. Notice, however that the experimental accuracy of solar observations is orders of magnitude better than that for any other star.

Nevertheless, the solar model itself already requires [44] $g_{a\gamma\gamma} \lesssim 10^{-9}\ \mathrm{GeV}^{-1}$, whereas the above Ge crystal bound has not yet reached such sensitivity. The $10^{-9}\ \mathrm{GeV}^{-1}$ limit sets a minimal

Table 1. Axion search sensitivities for experiments that are running (COSME [42] and DAMA [14]), being installed (CUORICINO [45] and ANAIS [4]) and planned (CUORE [4, 45] and GENIUS [46]) are compared with the result of SOLAX [41]. To estimate the best improvement that would be possible by selecting high-Z materials, a calculation for a Pb lattice is also shown. The coefficient K is defined in equation (3).

	K	M (kg)	b (counts keV^{-1} kg^{-1} day^{-1})	E_{th} (keV)	FWHM (keV)	$g^{lim}_{a\gamma\gamma}$(2 years) (GeV^{-1})
Ge [41]	2.5	1	3	4	1	2.7×10^{-9}
Ge [42]	2.3	0.234	0.7	3	0.4	2.4×10^{-9}
Ge [46]	2.5	1000	10^{-4}	4	1	3×10^{-10}
TeO_2 [45]	3.0	42	0.1	5	2	1.3×10^{-9}
TeO_2 [4, 45]	2.8	765	10^{-2}	3	2	6.3×10^{-10}
NaI [14]	2.7	87	1	2	2	1.4×10^{-9}
NaI [4]	2.8	107	2	4	2	1.6×10^{-9}
Pb	2.1	1000	10^{-4}	4	1	2.5×10^{-10}

goal for the sensitivity of future experiments, looking for axions with crystal detectors. We have carried out a prospective analysis of the potential for axion searches of various crystal detectors which are currently operating as dark matter detectors, such as crystals of germanium, tellurium oxide, sodium iodide and sapphire. From this analysis [42], it turns out that the sensitivity of an experimental axion search can be expressed as the upper bound of $g_{a\gamma\gamma}$ which such an experiment would provide from the non-appearance of the axion signal, for a given crystal, background and exposure. The ensuing limit on the axion–photon coupling $g^{lim}_{a\gamma\gamma}$ scales with the background and exposure in the following way:

$$g_{a\gamma\gamma} \leq g^{lim}_{a\gamma\gamma} \simeq K \left(\frac{b}{\text{counts keV}^{-1}\ \text{kg}^{-1}\ \text{day}^{-1}} \times \frac{\text{kg}}{M} \times \frac{\text{years}}{T} \right)^{\frac{1}{8}} \times 10^{-9}\ \text{GeV}^{-1} \tag{3}$$

where M is the total mass and b is the average background. The factor K depends on the parameters of the crystal, as well as on the experimental threshold and resolution.

The result is summarized in table 1, where the limit given by the germanium SOLAX experiment [41] is compared with those attainable with crystal detector experiments that are running [42, 14, 46], being installed [4, 45] and planned [4, 45, 46]. A Pb detector is also included, to give an indication of the best improvement that one would expect to gain by selecting heavy materials to take advantage of the proportionality to Z^2 of the cross section (crystals of $PbWO_4$ have been considered, for instance, in the CUORE set-up [45]). These results can be easily extended to other elements with lower atomic numbers than those considered in table 1 (for instance for detectors with Al_2O_3 and LiF crystals, which are also in operation or planned for use in dark matter experiments), although they are expected to yield less stringent limits. Figure 17 shows the expected axion signals for Primakov conversion in various crystals as a function of the time of the day.

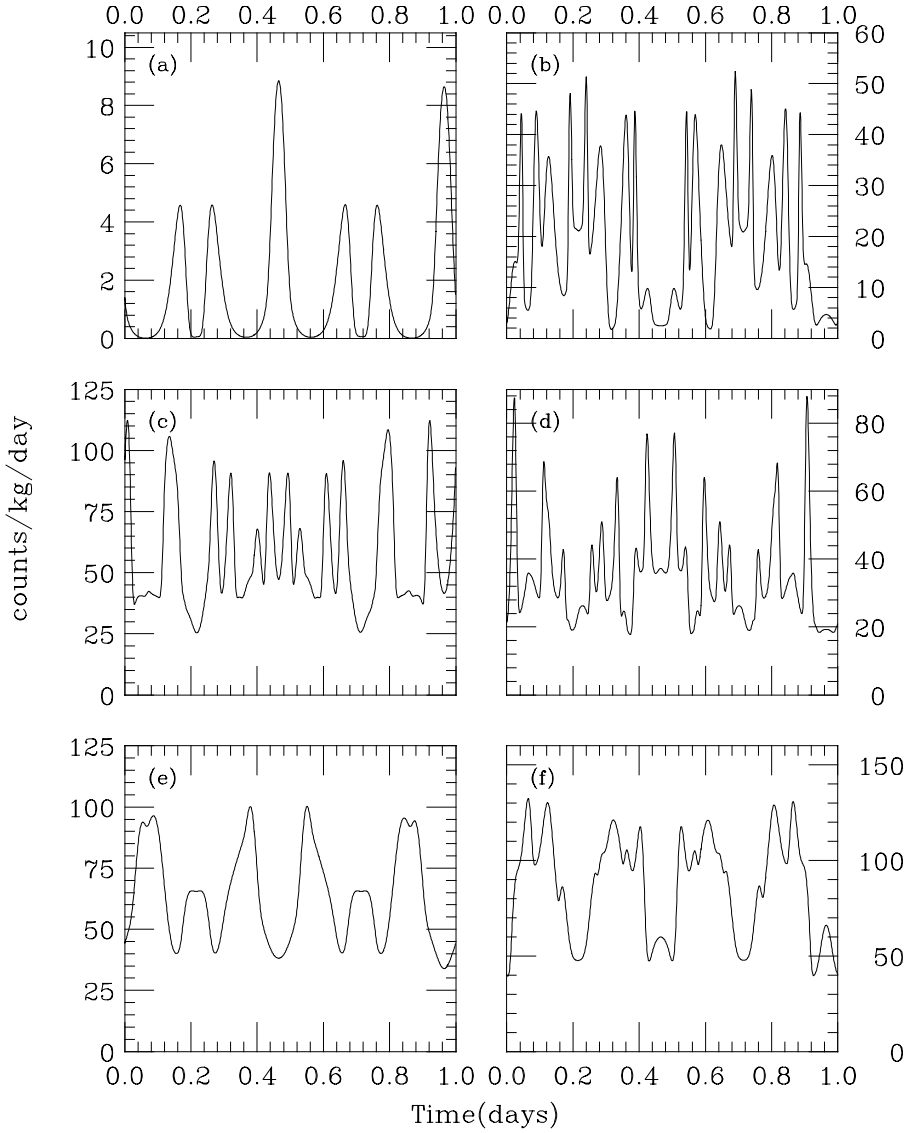

Figure 17. Expected axion signals for Primakov conversion in various crystals as a function of time for $\lambda = 1$. In the calculation the representative day of 1 April 1998 and the coordinates of the LNGS laboratory have been assumed: (a) Ge, 2 keV$\leq E_{ee} \leq$2.5 keV; (b) Ge, 4 keV$\leq E_{ee} \leq$4.5 keV; (c) TeO_2, 5 keV$\leq E_{ee} \leq$7 keV; (d) TeO_2, 7 keV$\leq E_{ee} \leq$9 keV; (e) NaI, 2 keV$\leq E_{ee} \leq$4 keV; and (f) NaI, 4 keV$\leq E_{ee} \leq$6 keV.

As shown in the expression for the $g_{a\gamma\gamma}$ bound of equation (3) the improvement in background and accumulation of statistics is washed out by the $\frac{1}{8}$ power dependence of $g_{a\gamma\gamma}$ on such parameters. It is evident, then, that detectors using crystals have no realistic chance of challenging the globular cluster limit. A discovery of the axion by this technique would presumably imply either a systematic error in the stellar-count observations in globular clusters or a substantial change in the theoretical models that describe the late stages of evolution of low-metallicity stars.

On the other hand, the sensitivity required for crystal detectors in order to investigate a range of $g_{a\gamma\gamma}$ compatible with the solar limit of [44] appears to be within reach, provided that improvements of background as well as a substantial increase in statistical power can be guaranteed. Collecting statistics of the order of a few ton years would not be so difficult to achieve by adding properly the results of various experiments. In such a case the investigation of a particular axion window that is not accessible to detectors of other types would only be a question of time, as a bonus from current and future dark matter searches.

Acknowledgments

The unpublished data presented here resulted from collaborative research with the following groups: IGEX (C Aalseth, F T Avignone, R L Brodzinski, W Hensley, I Kirpichnikov, A Klimenko, H Miley, S Osetrov, V Pogosov, J Reeves, A Smolnikov, A Tamanyan, A Vasenko and S Vasiliev), COSME (F T Avignone, R L Brodzinski and H Miley) and ROSEBUD (N Coron, G Dambier, P de Marcillac and J Leblanc). Results will be published in due course. The present work was partially supported by the CICYT under grant number AEN99-1033, the European Commission (DG-XII), grant ERB-FMRX-CT98-0167 and the USA–Spain Comisión Conjunta Hispano-Norteamericana de Cooperación Científica y Tecnológica.

References

[1] Jungman G, Kamionkowski M and Griest K 1996 *Phys. Rep.* **267** 195
[2] Morales A 1997 Dark matter and its detection *Summary talk at the NUPECC Workshop on the Present and Future of Neutrino Physics (Frascati, December 1997) (NUPECC Report on Highlights and Opportunities in Nuclear Physics)* ed J Vervier *et al* (`astro-ph/9810341`)
[3] For a recent survey of the status of WIMP searches, see, for instance
Morales A 2000 Direct detection of WIMP dark matter *Summary talk at the TAUP '99 Workshop (College de France, Paris, September 1999) Nucl. Phys.* B (Proc. Suppl.) **87** 477
[4] Morales A 1999 Selected projects in direct detection of dark matter *Proc. Neutrino Telescopes Workshop (Venice, February 1999)* ed M Baldo-Ceolin p 249
[5] Drukier A K *et al* 1986 *Phys. Rev.* D **33** 3495
[6] Morales J *et al* 1992 *Nucl. Instrum. Methods* A **321** 410
García E *et al* 1992 *Nucl. Phys.* B (Proc. Suppl.) **28A** 286
García E *et al* 1995 *Phys. Rev.* D **51** 1458
[7] Aalseth C *et al* 1999 *Phys. Rev.* C **59** 2108
González D *et al* 2000 *Proc. TAUP '99 Workshop (College de France, Paris, September 1999) Nucl. Phys.* B (Proc. Suppl.) **87** 278
[8] Caldwell D O *et al* 1988 *Phys. Rev. Lett.* **61** 510
[9] Reusser D *et al* 1991 *Phys. Lett.* B **255** 143
[10] Drukier A K *et al* 1992 *Nucl. Phys.* B. (Proc. Suppl.) **28A** 293
[11] Baudis L *et al* 1999 *Phys. Rev.* D **59** 022001
[12] Abriola D *et al* 1996 *Astropart. Phys.* **6** 63
[13] Bernabei R *et al* 1996 *Phys. Lett.* B **379** 299
[14] Bernabei R *et al* 1998 *Phys. Lett.* **424** 195
Bernabei R *et al* 1996 *Phys. Lett.* B **450** 448
[15] Sarsa M L *et al Nucl. Phys.* B (Proc. Suppl.) **48** 73
Sarsa M L *et al* 1996 *Phys. Lett.* B **386** 458

Sarsa M L *et al* 1997 *Phys. Rev.* D **56** 1856
[16] Freese K *et al* 1988 *Phys. Rev.* D **37** 3388
[17] Sarsa M L *et al* 1994 *Nucl. Phys.* B (Proc. Suppl.) **35** 154
[18] Belli P *et al* 1996 *Nuovo Cimento* C **19** 537
[19] Abriola D *et al* 1999 *Astropart. Phys.* **10** 133
[20] Fushimi K *et al* 1999 *Astropart. Phys.* **12** 185
[21] Fushimi K *et al* 1993 *Phys. Rev.* C **47** R425
[22] Engel J 1991 *Phys. Lett.* B **264** 114
[23] Ellis J and Flores R A 1993 *Nucl. Phys.* **B400** 125
[24] Iachelo F *et al* 1991 *Phys. Lett.* B **254** 220
[25] Gerbier G *et al* 1999 *Astropart. Phys.* **11** 287
[26] Cebrián S *et al* 1999 Sensitivity plots for WIMP direct detection using the annual modulation signature (`hep-ph/9912394`)
[27] See for instance
Booth N, Cabrera B and Fiorini E 1996 *Ann. Rev. Nucl. Sci.* **46** 471
[28] Berge L *et al* 1999 *Nucl. Phys.* B (Proc. Suppl.) **70** 69
Chardin G 2000 Status of the EDELWEISS experiment *Proc. TAUP' 99 Workshop (College de France, Paris, September 1999) Nucl. Phys.* B (Proc. Suppl.) **87** 74
[29] Abusaidi R *et al* Exclusion limits on the WIMP-nucleon cross-section from the CDMS (`astro-ph/0002471`) and references therein
[30] de Marcillac P *et al* 1993 *Nucl. Instrum. Methods* A **337** 95
[31] Bobin C *et al* 1999 *Nucl. Phys.* B (Proc. Suppl.) **70** 90
[32] Cebrián S *et al* 1999 *Astropart. Phys.* **10** 361
[33] Zhou J W *et al* 1994 *Nucl. Instrum. Methods* A **349** 225
[34] Gabutti A *et al* 1996 *Astropart. Phys.* **6** 1
[35] Peccei R D and Quinn H R 1977 *Phys. Rev. Lett.* **38** 1440
[36] Kolb E W and Turner M S 1990 *The Early Universe* (Reading, MA: Addison-Wesley)
[37] Burrows A, Ressel M T and Turner M S 1990 *Phys. Rev.* D **42** 3297
[38] Engel J, Seckel D and Hayes A C 1990 *Phys. Rev. Lett.* **65** 960
[39] Pascos E A and Zioutas K 1994 *Phys. Lett.* B **323** 367
[40] Creswick R J, Avignone F T III, Farach H A, Collar J I, Gattone A O, Nussinov S and Zioutas K 1998 *Phys. Lett.* B **427** 235
[41] Gattone A O *et al* (The SOLAX collaboration) 1998 *Phys. Rev. Lett.* **81** 5071
[42] Cebrián S *et al* 1999 *Astropart. Phys.* **10** 397
Irastorza I G 2000 Prospects for solar axion searches with crystals via Bragg scattering *Proc. TAUP '99 Workshop (College de France, Paris, September 1999) Nucl. Phys.* B (Proc. Suppl.) **87** 102
[43] Raffelt G 1996 *Stars as Laboratories for Fundamental Physics* (Chicago: University of Chicago Press)
Raffelt G and Dearborn D 1987 *Phys. Rev.* D **36** 2211
[44] Schlattl H, Weiss A and Raffelt G *Astropart. Phys.* submitted (`hep-ph/9807476`)
[45] Alessandrello A *et al* 2000 *Proc. TAUP '99 Workshop (College de France, Paris, September 1999) Nucl. Phys.* B (Proc. Suppl.) **87** 78
[46] Baudis L *et al* 1999 *Nucl. Instrum. Methods* A **426** 425